The Cryosphere Discuss., https://doi.org/10.5194/tc-2017-251
Manuscript under review for journal The Cryosphere
Discussion started: 12 February 2018
© Author(s) 2018. CC BY 4.0 License.

The Cryosphere Discussions
Open Access
EGU

Ice velocity of Jakobshavn Isbræ, Petermann Glacier, Nioghalvfjerdsfjorden and Zachariæ Isstrøm, 2015-2017, from Sentinel 1-a/b SAR imagery

Adriano Lemos[1], Andrew Shepherd[1], Malcolm McMillan[1], Anna E. Hogg[1], Emma Hatton[1], Ian Joughin[2]

[1]Centre for Polar Observation and Modelling, University of Leeds, Leeds, United Kingdom
[2]Polar Science Center, Applied Physics Laboratory, University of Washington, Seattle, Washington, USA

Correspondence to: Adriano Lemos (A.G.Lemos14@leeds.ac.uk)

Abstract

Systematically monitoring Greenland's outlet glaciers is central to understanding the timescales over which their flow and sea level contributions evolve. In this study we use data from the new Sentinel-1a/b satellite constellation to generate 187 velocity maps, covering 4 key outlet glaciers in Greenland; Jakobshavn Isbræ, Petermann Glacier, Nioghalvfjerdsfjorden and Zachariæ Isstrøm. These data provide a new high temporal resolution record of each glacier's evolution since 2014, and resolve recent seasonal and inter-annual changes in Greenland outlet glacier speed with an estimated certainty of 10 %. We find that since 2012, Jakobshavn Isbræ has been decelerating, and now flows approximately 1250 m yr^{-1} (10 %) slower than 5 years previously, thus reversing an increasing trend in ice velocity that has persisted during the last decade. Despite this, we show that seasonal variability in ice velocity remains significant; up to 750 m yr^{-1} (14 %) at a distance of 12 km inland of the terminus. We also use our new dataset to demonstrate a strong relationship between ice front position and ice flow at Jakobshavn Isbræ, with increases in speed of ~1800 m yr^{-1} in response to 1 km of retreat. Elsewhere, we record significant seasonal changes in flow of up to 25 % and 18 % at Petermann Glacier and Zachariæ Isstrøm, respectively. This study provides a first demonstration of the capacity of a new era of operational radar satellites to provide frequent, and timely, monitoring of ice sheet flow, and to better resolve the timescales over which glacier dynamics evolve.

1. Introduction

Between 1992 and 2011, the Greenland Ice Sheet lost mass at an average rate of 142±49 Gt yr^{-1} [Shepherd et al., 2012], increasing to 269±51 Gt yr^{-1} between 2011 and 2014 [McMillan et al., 2016]. Ice sheet mass balance is determined from the ratio of surface mass input and ice discharge exported from the ice sheet [van den Broeke et al., 2009]. In 2005, dynamic imbalance was responsible for roughly two-thirds of Greenland's total mass balance, making an important contribution to freshwater input into the ocean and 0.34 mm yr^{-1} to the global sea level rise at that time [Rignot and Kanagaratnam, 2006]. Despite the anomalous atmospheric warming events, especially during 2012 [Tedesco et al., 2013], and therefore more spatially extensive and longer lasting surface melt during this period, marine-terminating outlet glaciers in Greenland still contributes roughly 30 % (2000–2012) of total mass loss [Enderlin et al., 2014]. The observed acceleration of many marine-based glaciers in the western and northern regions of Greenland over the last years may have been driven by rises in air and adjacent ocean temperatures, which enhanced the surface melting and erosion of their termini [Holland et al., 2008; Moon et al, 2014; Moon et al., 2015]. The associated increases in basal sliding and calving of their ice fronts in turn produce enhanced discharge, leading to dynamical imbalance and additional ice loss [Joughin et al., 2010; Joughin et al., 2014]. Acceleration of marine-terminating glaciers is, however, highly variable in space and time [Howat et al., 2010; Moon et al., 2012; Enderlin et al., 2014], due to the geometry of individual glaciers, and the high frequency variability in the forcing mechanisms. This complexity in glacier response challenges efforts to model their future evolution [Joughin et al., 2012; Bondzio

The Cryosphere Discuss., https://doi.org/10.5194/tc-2017-251
Manuscript under review for journal The Cryosphere
Discussion started: 12 February 2018
© Author(s) 2018. CC BY 4.0 License.

et al., 2017] and, therefore, frequent and systematic monitoring is essential to understand the processes governing their dynamic stability and contribution so future mean sea level rise [Joughin et al., 2010; Shepherd et al., 2012].

Ice motion measurements are essential for monitoring ice sheet dynamics, ice discharge and for assessing an ice sheet's mass budget [Joughin et al., 1995]. At present, the only way to monitor ice velocity at a continental scale is through satellite imagery. Glacier velocities were first measured using Landsat satellite data acquired during the 1970s through digital optical image comparison [Lucchitta & Ferguson, 1986]. However, due to the dependency upon daylight conditions and the limited acquisitions across the Polar Regions, the use of Synthetic Aperture Radar (SAR) images has become common since the launch of ERS-1 in 1991. In the following decades, these data have been used to monitor dynamic processes occurring across remote areas such as the Greenland and Antarctic ice sheets [Joughin et al., 2010; Rignot & Mouginot, 2012; Nagler et al., 2015 Mouginot et al., 2017]. More recently, after the launch by the European Space Agency (ESA) of the Sentinel 1-a and 1-b satellites, in April 2014 and April 2016 respectively, many key ice margin areas are systematically monitored every 6 to 12 days. This novel dataset provides the opportunity to systematically monitor the dynamical process driving glacier ice velocity over periodic and short temporal scales. Here we use the Sentinel SAR archive to investigate the temporal variation in ice flow since October 2014 at four large outlet glaciers of the Greenland ice sheet.

2. Study areas

In this study, we map ice velocity of the Jakobshavn Isbræ (JI), Petermann Glacier (PG), Nioghalvfjerdsfjorden (79-G) and Zachariæ Isstrøm (ZI), which are four of the largest marine-based ice streams in Greenland and combined contain ice equivalent to 1.8 m of global sea-level rise [Mouginot et al., 2015; Jensen et al., 2016].

Jakobshavn Isbræ terminates in the Ilulissat Icefjord in western Greenland (Figure 1a), and is the fastest glacier draining the ice sheet [Enderlin et al., 2014; Joughin et al., 2014]. During the late 1990s, the ice tongue experienced successive breakup events and the glacier began to speedup, exhibiting annual increases in speed of 7 % per year from 2004 and 2007 [Joughin et al., 2008a; Joughin et al., 2012; Joughin et al., 2014]. Over the last few years, the speed up has continued, reaching maximum velocities in excess of 17 km yr^{-1} during 2012 and 2013 [Joughin et al., 2012; Joughin et al., 2014]. It has been suggested [Tedesco et al., 2013] that the speedup over this period was enhanced by anomalously high melting across the ice sheet surface. Jakobshavn Isbræ is susceptible to changes in the adjacent ocean and Holland et al. [2008] have shown that warm water originating in the Irminger Sea likely enhanced basal melting and weakened the floating ice tongue, triggering its break up in 1997. Furthermore, Gladish et al. [2015] showed that subsequent changes which, occurred between 2001–2014, were mainly triggered by changes in Ilulissat Icefjord water temperatures adjacent to the glacier. At present, JI is a tidewater glacier and has a bimodal behaviour, retreating by ~3 km during summer and advancing by a similar amount during winter seasons [Cassotto et al., 2016]. Therefore, as showed by Jensen et al. [2016] through analysis of optical images from 1999 to 2013, it has not exhibited an unusually large change in area (-10.3 km^2 yr^{-1}).

Petermann Glacier flows into the Hall Basin in the Nares Strait in Northwest Greenland (Figure 1b), and has a perennial floating ice tongue of 1280 km^2 in area [Hogg et al, 2016]. PG is grounded on bedrock ~300 m below sea level and, therefore, is also influenced by the adjacent ocean [Münchow et al, 2014; Hogg et al., 2016]. The retreat of the ice stream calving front led to an area decrease of 352 km^2 from 1959 to 2008, 270 km^2 in 2010 and 130 km^2 in 2012 [Johannessen et al., 2013]. It is considered a dynamically stable marine-terminating glacier despite several grounding line advancing and retreating events between 1992 and 2011, with a

The Cryosphere Discuss., https://doi.org/10.5194/tc-2017-251
Manuscript under review for journal The Cryosphere
Discussion started: 12 February 2018
© Author(s) 2018. CC BY 4.0 License.

migration rate of 25.2 m a^{-1} [Hogg et al., 2016]. PG has an average velocity of ~1100 m yr^{-1} at its grounding line since the 1990s [Rignot, 1996; Rignot & Steffen, 2008] and a multi-annual trend (2006–2010) in flow speed of 30 m yr^{-2} [Nick et al., 2012]. The ice shelf is thicker than 100 m and it is 15 km wide, with low resistive stresses along flow due to the limited attachment to the fjord walls, diminishing the velocity response after calving events [Nick et al., 2012].

Nioghalvfjerdsfjorden and Zachariæ Isstrøm are situated in the northeast of Greenland (Figure 1c and Figure 1d respectively). The two glaciers together drain more than 10 % of the Greenland Ice Sheet [Rignot & Mouginot, 2012], and their maximum velocities are found near the grounding line. Although located in the same region they have, in recent years, exhibited different behaviour. 79-G underwent a modest velocity increase of ~150 m yr^{-1} between 2001 and 2011 at the grounding line [Khan et al., 2014]. In contrast, during the same period, ZI exhibited a much larger increase in speed greater than 600 m yr^{-1} [Khan et al., 2014]. The ice thinning rates above the grounding line varies from 5.1 m yr^{-1} in ZI (2010–2014) to 1.4 m yr^{-1} in 79-G (2012–2014) [Mouginot et al., 2015]. Between 1999 and 2013, ZI has undergone an average area change of -26.0 km^2 yr^{-1}, due to break off of the ice tongue and is now a tidewater glacier [Khan et al., 2014; Jensen et al., 2016]. In contrast, 79-G had a much lower average area change during the same period of -4.7 km^2 yr^{-1} and still retains a small ice shelf [Jensen et al., 2016], although recent ice shelf thinning [Mouginot et al., 2015] may increase vulnerability to break up in the future.

3. Data and Methodology

To map ice velocity, we used Single Look Complex (SLC) Synthetic Aperture Radar images acquired in the Interferometric Wide swath (IW) mode from the Sentinel-1a and Sentinel-1b satellites. Data were acquired in the period spanning from October 2014 to February 2017 and from October 2016 to February 2017, for Sentinel-1a and Sentinel-1b respectively (Table S1). Each satellite has a repeat cycle of 12 days and 180 degrees orbital phasing difference, resulting in a revisit time of 6 days over the same area after the Sentinel-1b launch. The Sentinel SAR instruments operate at C-Band, with a centre frequency of 5.405 GHz, corresponding to a wavelength of 5.55 cm. The IW mode has a 250 km swath and spatial resolution of 5 m in ground range and 20 m in azimuth. It has burst synchronization for interferometry and acquires data in 3 sub-swaths, each containing a series of bursts, which are acquired using the Terrain Observation with Progressive Scans SAR (TOPSAR) imaging technique [Yague-Martinez et al., 2016]. We followed the workflow described below to derive 187 ice velocity maps from pairs of Sentinel-1a/b SAR images over Jakobshavn Isbræ, Petermann Glacier, Nioghalvfjerdsfjorden and Zachariæ Isstrøm, using the GAMMA-SAR software [Gamma Remote Sensing, 2016].

We used the SAR intensity tracking technique [Strozzi et al., 2002] to estimate surface ice velocities due to glacier flow, assuming that the ice flow occurs parallel to the surface. This method uses a cross correlation algorithm applied to image patches [Strozzi et al. 2002; Pritchard et al. 2005, Paul et al. 2015] to estimate offsets between similar features, such as crevasses and radar speckle patterns, in two co-registered SAR images (Table S1). Images were co-registered using the precise orbit information, available 20 days after the image acquisition, establishing a position accuracy of 5 cm [Sentinels POD team, 2013]. The elimination of the orbital offsets isolates displacement due to the glacier movement [Strozzi et al., 2002]. To estimate ice flow, we then used windows sizes of 350 pixels in ground range (~ 1.7 km) and 75 pixels in azimuth (~1.5 km) for each glacier, to produce a series of velocity maps with spatial resolution of 388 m in ground range and 320 m in azimuth.

Image matches with low certainty, defined as returning a normalised cross-correlation of less than 0.05, were rejected and the results were then converted into displacement in ground range coordinates using the Greenland Ice Mapping Project (GIMP) digital elevation model (DEM) posted on a 90 m grid [Howat, 2014]. Along- and across-track displacement components were combined

© Author(s) 2018. CC BY 4.0 License.

to determine the displacement magnitude, which was then converted to an estimate of annual velocity using the temporal baseline of each image pair. Final velocity products were posted on 100 m by 100 m grids. Post-processing of ice velocity data reduces noise and removes outliers [Paul et al., 2015], so we applied a low-pass filter (moving mean) twice to the data, using a kernel of 1 km by 1 km, and we reject values where the deviation between the unfiltered and filtered velocity magnitude exceeds 30 %. We apply a labelling algorithm to identify and classify regions with similar values, excluding isolated pixels with a non-coherent area of velocity values, or where the area of the classified region was smaller than 1/1000th of the processed image size.

Errors in our velocity estimates arise primarily through inexact co-registration of the SAR images, uncertainties in the digital elevation model used in the terrain correction, and fluctuations in ionospheric activity and tropospheric water vapour [Nagler et al., 2015; Hogg et al., 2017]. To estimate the accuracy of our Sentinel-1 average velocity data (Figure 1 and Figure 3) we computed pixel-by-pixel errors based on the signal to noise ratio (SNR) of the cross correlation function [Hogg et al., 2017]. We then averaged these estimates across all images in our temporal stack to determine the percentage errors associated with our mean velocity maps (Figure 3). Although in isolated areas the error exceeds 30 %, the mean error across the whole imaged area were approximately 10 % for JI, 7 % for PG, and 8 % for 79G and ZI, with all four glaciers exhibiting higher errors across their faster flowing and steeper areas. Where localised rates of surface elevation change are high, the surface slope may have evolved away from that of the GIMP DEM used in our processing. To assess the sensitivity of our velocity estimates to this effect, we selected the JI site where thinning is most pronounced, and used airborne estimates of elevation change to update the DEM. We find that in this extreme case, the large thinning rates may introduce an additional uncertainty of 200-300 m yr^{-1} within individual pixels of our velocity estimates, albeit limited to the first 10 km upstream of the grounding line (Table S2). Over floating ice tongues, uncompensated vertical tidal displacement may also introduce additional uncertainty into our velocity fields. The sensitivity of our results to this effect was assessed based upon a net 50 cm tidal displacement over 6-12 day repeat period and a centre swath incidence angle of 35 degrees. We estimate that such a tidal signal would introduce ~20–40 m yr^{-1} additional uncertainty into the ground range component of our velocity fields. In the context of this study, this uncertainty does not affect the results at JI or ZI, and it is limited only to the floating sections of PG and 79G.

To provide an independent evaluation of our ice velocity dataset, we finally compared them (Table S1) to independent estimates derived from TerraSAR-X (TSX) SAR imagery, which has a repeat period acquisition of 11 days and spatial resolution up to 3 m [Joughin et al., 2016]. The TSX data consist of 444 image pairs covering Jakobshavn Isbræ over the period January 2009 to January 2017, 18 pairs at Petermann Glacier over the period November 2010 to December 2016, and 17 pairs at Nioghalvfjerdsfjorden over the period March 2011 to December 2016. In general, the temporal evolution of the S1-a/b measurements matches very closely with the TSX estimates (Figure 4b and Figure 4c). At JI, we are able to compare S1 and TSX datasets at three different locations to assess their consistency (Figure 4). Even though the flow speed at these sites is high, which typically proves more challenging for feature tracking techniques, we find good agreement between the two datasets, especially at the J1 and J2 sites, with mean differences of 40 m yr^{-1} and 76 m yr^{-1} respectively. However, nearer to the calving front (site Jif), the S1-a/b measurements tend to give significantly higher velocities than TSX with a mean difference of 489 m yr^{-1} (5 % of the mean velocity) between the two datasets.

4. Results and Discussion

We used our complete Sentinel-1a/b dataset (Table S1) to generate contemporary, time-averaged velocity fields at each of our study sites (Figure 1). To investigate spatial and temporal variations in ice velocity, we then extracted profiles in the along- and across-flow directions, together with time series at fixed glacier locations (Figure 1). Our velocity profiles in Jakobshavn Isbræ, Petermann Glacier, Nioghalvfjerdsfjorden and Zachariæ Isstrøm reached maximum mean speeds of approximately 9 km yr^{-1}, 1.2 km yr^{-1}, 1.4 km yr^{-1}, 2.7 km yr^{-1}, respectively. The location of the velocity magnitude varied between glaciers, as a result of their differing

© Author(s) 2018. CC BY 4.0 License.

geometries. For JI and ZI, neither of which have a significant floating tongue, we find a progressive increase in ice velocity towards the calving front. For PG, the maximum velocity is reached at the grounding line and remains steady along the ice tongue (~46 km extension in Figure 2b). In contrast, although 79G also reaches its maximum velocity close to the grounding line, its speed then diminishes by ~ 50 % (Figure 2c) near the ice front location where the ice flow divides into two main portions before it reaches several islands and ice rises (Figure S1b). Furthermore, it is interesting to note that, despite being located in the same region, the adjacent glacier ZI flows ~60 % faster in comparison. JI, PG and ZI glaciers show velocity increases progressively downstream across the transverse profiles. The four glaciers, JI, PG, 79G and ZI respectively reduce in speed to half of their maximum velocity at distances of 12 km, 22 km, 18 km, and 12 km inland of their grounding lines, highlighting the importance of resolving glacier velocities within their near terminus regions.

Next, we used the Sentinel-1a/b and TerraSAR-X velocities to assess the seasonal and longer-term variations in Jakobshavn Isbræ ice velocity over the period 2009–2017. Our Sentinel-1a/b velocity estimates at JI resolve clear seasonal velocity fluctuations, superimposed upon longer term decadal scale variability, continuing observations made by previous satellite instruments [Joughin et al., 2012; Joughin et al., 2014]. At site J1 we find an average summer increase in speed of 750 m yr^{-1}, or 14 %. Inland, the amplitude of seasonal variability diminishes, to an average of 300 m yr^{-1} (8 %) at J2. Our near-continuous, decadal-scale record clearly shows that the amplitude of the seasonal signal has evolved through time. At J1, for example, the average seasonal variability in ice speed was 400 m yr^{-1} during 2009-2011, increasing by more than a factor of 3, to 1400 m yr^{-1} between 2012 and 2013 and then diminishing to 750 m yr^{-1} between 2015–2017.

Turning to the longer term evolution of JI (Figure 5; time series location shown in Figure 1), fitting a linear trend to the data suggests an annual acceleration since 2009 of ~218 m yr^{-1} at Jif, diminishing inland to ~128 m yr^{-2} at J1, and ~102 m yr^{-2} at J2. Although this provides a simple characterisation of the longer-term evolution in ice speed, it is clear from our time series that computing a linear trend does not capture the full decadal scale variability in ice velocity. In particular, we note that much of the acceleration occurred between 2011 and 2013, and since then there has been a notable absence of multi-annual acceleration as earlier records suggest [Joughin et al., 2014]. Computing trends in ice velocity since 2012, for example, shows a modest decline in speed of 321m yr^{-2} over the 5-year period. Because calving front migration has been suggested as a driver of JI velocity fluctuations [Joughin et al., 2008a; 2008b; Bondzio et al., 2017], we used our observations of calving front position to assess the correlation between ice speed and calving front location, relative to their respective long term means (Figure 6). Based on the linear regression, our dataset indicates correlation coefficients (R^2) of 0.62 (2009–2011) and 0.79 (2012–2017), and velocity changes by 1100 and 1600 m yr^{-1} per kilometre of calving front retreat, respectively.

At Petermann Glacier we extracted two velocity time series at P1, located ~45 km downstream of the grounding line and close to the calving front of the ice tongue; and P2, ~10 km upstream of the grounding line. These locations were chosen to examine any differences in velocity evolution over the grounded and floating portions of the glacier. Our P1 time series starts early 2015 because it is not covered by the TerraSAR-X dataset (Figure 7a). We observe that, in general, ice at P1 flows ~400 m yr^{-1} faster than P2. Fitting a linear trend to the longer P2 dataset indicates no significant trend in ice velocity since 2011, although the precision of this trend is hampered by the sparse data coverage during the early part of this period. Continued monitoring by Sentinel-1 will improve our confidence in resolving any decadal scale variability. The improvement in temporal sampling provided by Sentinel-1 at this site is clear (Figure 7a) and allows us to resolve the seasonal cycle in velocity since 2015. At P1, we detect a seasonal change in speed of ~ 300 m yr^{-1}, equivalent to a 25 % increase relative to its winter velocity. This provides further evidence of a seasonal velocity cycle which has been observed at both Petermann and other glaciers in this region, and is understood to be predominantly controlled by changes in basal traction, induced by penetration of surface melt water to the bed [Nick et al., 2012; Moon et al., 2014; Moon et al., 2015]. This is further supported by our analysis of changes in calving front position (Figure S1a) which shows that, in contrast to JI, seasonal acceleration does not coincide with ice front retreat. Specifically, we found that during the summers of 2015 and

© Author(s) 2018. CC BY 4.0 License.

2016, the calving front of PG advanced ~1 km during the speedup (Figure S1a). These observations are consistent with previous modelling results, which did not find evidence of acceleration driven by large calving events in 2010 and 2012 [Nick et al., 2012; Münchon et al., 2014], suggesting that the ice shelf exerts low backstress on the glacier. More recently, we note that since September 2016 PG has developed a new crack near the ice front, which has continued to grow in length up to the present day.

At 79-G, we again extracted velocity time series over the ice shelf (F1, ~20 km downstream of the grounding line) and at the grounding line (F2). In contrast to PG and due to the steeper surface gradient upstream of the grounding line (Figure 2c), ice flow is slower on the floating tongue than at the grounding line location (Figure 7b). We observe a seasonal speed up of ~10 % at F2 during summer 2016, although evidence of the same acceleration on the ice shelf is not clear given the magnitude of the signal and the precision of our data. Fitting a linear trend to our data returns an annual change in velocity of 15 m yr^{-2} since 2011, although assessing the significance of this result is difficult given the limited data sampling early in the period. Turning to Zachariæ Isstrøm, we extract time series at two locations slightly upstream of the grounding line in order to observe different temporal responses between them (Figure 7c). At this glacier, no observations are available within the TSX dataset and so our time series is limited to the period December 2015 to January 2017. Nonetheless, like its neighbour ZI, we again find evidence of a summer speed up during 2016, equating to around 400 m yr^{-1}, or 18 %. Given the short period of observations we do not attempt to derive a longer-term trend in ice velocity at this site.

We compared our estimates to the results of previous studies to assess the level of agreement relative to past work. At Petermann, we have observed increases in ice velocity of ~10 % at P1 and ~8 % at P2 between the 2015/2016 and 2016/2017 winters, matching in percentage with the observations made during the same period by Münchon et al. [2016]. Furthermore, the Sentinel-1a/b dataset indicates a multi-annual acceleration of ~32 m/yr^2 between 2015-2017 at P1, which is similar to the ~30 m/yr^2 reported by Nick et al. [2012] based upon observational measurements over a longer period, from 2006 to 2010. The same authors also show seasonal variations of ~20–25 % over the same location, similar to the ~22 % shown by the Sentinel-1 dataset. At 79-G, Mouginot et al. [2015] showed a speedup of 8 % from 1976 to 2014 with the main changes occurring after 2006, similar to our estimates which also suggest a slight multi-year trend of ~16 m yr^{-2} (~8 %) for F2 between 2015 and 2017. Zachariæ Isstrøm shows seasonal variation up to 15 % between 2015 and 2017 in the Sentinel-1 dataset, agreeing with seasonal variation up to 20 % estimated by Mouginot et al. [2017] using Landsat-8 optical images during 2014–2016.

6 Conclusions

We have presented a new, high temporal resolution record of ice velocity evolution for four important marine based glaciers in Greenland, updated to the present day (February 2017). Using SAR data acquired by the Sentinel-1a/b constellation, with its 250 km wide swath and frequent revisit time, we have produced 187 velocity maps, which, in combination with 479 maps from the TerraSAR-X satellite, provide detailed spatial and temporal coverage of these key sites. Importantly, the systematic acquisition cycle of Sentinel-1a/b, which now provides measurements of all of these sites every 6 days allows for detailed monitoring of both seasonal and multi-annual velocity fluctuations. The short revisit time of 6 days, made possible since the launch of Sentinel-1b in April 2016, particularly benefits the retrieval of velocity signals across fast flowing regions close to the ice front, due to a reduction in the decorrelation occurring between image pairs. Using this new dataset, we confirm evidence of intra-annual variations in ice velocity and clear seasonal cycles occurring over the past few years at JI, PG, 79G and ZI. Of the sites studied here, JI exhibits the largest velocity variations, as demonstrated in other studies, which we show are strongly correlated with the evolution of the position of its calving front. Notably, however, in the last 5 years the longer-term ice speed has started to decreased. This study demonstrates the utility of a new era of operational SAR imaging satellites for building systematic records of ice sheet outlet glacier velocity and

© Author(s) 2018. CC BY 4.0 License.

its good agreement with TerraSAR-X products, which indicates Sentinel-1 can confidently extend the times series that began with other sensors. Looking to the future, these datasets are key for the timely identification of emerging signals of dynamic imbalance, and for understanding the processes driving ice velocity change.

Competing interests. The authors declare that they have no conflicts of interest.

Acknowledgements: This work was led by the NERC Centre for Polar Observation and Modelling, supported by the Natural Environment Research Council (cpom300001), with the support of a grant (4000107503/13/I-BG), and the European Space Agency. AEH is funded from the European Space Agency's support to Science Element program, and an independent research fellowship (4000112797/15/I-SBo). A.L. was supported by CAPES-Brazil PhD scholarship. The NASA MEaSUREs program (NASA grants NNX08AL98A and NNX13AI21A) supported I.J.'s contribution. All data is freely available for download at http://www.cpom.ucl.ac.uk/csopr/iv/.

© Author(s) 2018. CC BY 4.0 License.

6 References

Bondzio, J. H., Morlighem, M., Seroussi, H., Kleiner, T., Rückamp, M., Mouginot, J., Humbert, A. (2017). The mechanisms behind Jakobshavn Isbrae's acceleration and mass loss: a 3D thermomechanical model study. Geophysical Research Letters, 44, 6252–6260. https://doi.org/10.1002/2017GL073309

Cassotto, R., Fahnestock, M., Amundson, J. M., Truffer, M., & Joughin, I. (2015). Seasonal and interannual variations in ice melange and its impact on terminus stability, Jakobshavn Isbræ, Greenland. Journal of Glaciology, 61(225), 76–88. https://doi.org/10.3189/2015JoG13J235

Enderlin, E. M., Howat, I. M., Jeong, S., Noh, M.-J., Angelen, J. H. van, & van den Broeke, M. R. (2014). An improved mass budget for the Greenland ice sheet. Geophys. Res. Lett., 41, 1–7. https://doi.org/10.1002/2013GL059010.

European Space Agency (ESA) Greenland Ice Sheet Climate Change Initiative (CCI) project (2017). Greenland calving front locations v.3.0. http://products.esa-icesheets-cci.org/products/details/greenland_calving_front_locations_v3_0.zip/.

GAMMA REMOTE SENSING. (2015). Sentinel-1 processing with GAMMA software. Version 1.2.

Gladish, C. V., Holland, D. M., Rosing-Asvid, A., Behrens, J. W., & Boje, J. (2015). Oceanic Boundary Conditions for Jakobshavn Glacier. Part II: Provenance and Sources of Variability of Disko Bay and Ilulissat Icefjord Waters, 1990-- 2011. Journal of Physical Oceanography, 45(2003), 33–63. https://doi.org/10.1175/JPO-D-14-0045.1

Hogg, A. E., Shepherd, A., Cornford, S. L., Briggs, K. H., Gourmelen, N., Graham, J., Wuite, J. (2017). Increased ice flow in Western Palmer Land linked to ocean melting. Geophys. Res. Lett., (44), 1–9. doi: 10.1002/2016GL072110

Hogg, A. E., Shepherd, A., Gourmelen, N., & Engdahl, M. (2016). Grounding line migration from 1992 to 2011 on Petermann Glacier, North-West Greenland. Journal of Glaciology, 1–11. https://doi.org/10.1017/jog.2016.83

Holland, D. M., Thomas, R. H., Young, B. De, Ribergaard, M. H., & Lyberth, B. (2008). Acceleration of Jakobshavn Isbræ triggered by warm subsurface ocean waters. Nature Geoscience, 1, 1–6. https://doi. 10.1038/ngeo316

Howat, I. M., Negrete, a., & Smith, B. E. (2014). The Greenland Ice Mapping Project (GIMP) land classification and surface elevation data sets. The Cryosphere, 8(4), 1509–1518. https://doi.org/10.5194/tc-8-1509-2014

Jensen, T. S., Box, J. E., & Hvidberg, C. S. (2016). A sensitivity study of annual area change for Greenland ice sheet marine terminating outlet glaciers: 1999–2013. Journal of Glaciology, 1–10. https://doi.org/10.1017/jog.2016.12

Johannessen, O. M., Babiker, M., & Miles, M. W. (2013). Unprecedented Retreat in a 50-Year Observational Record for Petermann. Atmospheric and Oceanic Science Letters, 6(5), 259–265. https://doi.org/10.3878/j.issn.1674-2834.13.0021.1

Joughin, I., Smith, B. E., Shean, D. E., & Floricioiu, D. (2014). Brief communication: Further summer speedup of Jakobshavn Isbræ. Cryosphere, 8(1), 209–214. https://doi.org/10.5194/tc-8-209-2014

Joughin, I. (2002). Ice-sheet velocity mapping: a combined interferometric and speckle-tracking approach. Annals of Glaciology, 34(1), 195–201. https://doi.org/10.3189/172756402781817978

Joughin, I., Howat, I. M., Fahnestock, M., Smith, B., Krabill, W., Alley, R. B., Truffer, M. (2008a). Continued evolution of Jakobshavn Isbræ following its rapid speedup. Journal of Geophysical Research: Earth Surface, 113(4), 1–14. https://doi.org/10.1029/2008JF001023

© Author(s) 2018. CC BY 4.0 License.

Joughin, I., Das, S. B., King, M. A., Smith, B. E., Howat, I. M., & Moon, T. (2008b). Seasonal Speedup Along the Western Flank of the Greenland Ice Sheet. Science, 320(April), 781–784. https://doi.org/10.1126/science.1153288

Joughin, I., Smith, B., Howat, I., & Scambos, T. (2016). MEaSUREs Multi-year Greenland Ice Sheet Velocity Mosaic, Version 1. Boulder, Colorado USA. NASA National Snow and Ice Data Center Distributed Active Archive Center. Retrieved from http://dx.doi.org/10.5067/QUA5Q9SVMSJG

Joughin, I., Smith, B. E., Howat, I. M., Floricioiu, D., Alley, R. B., Truffer, M., & Fahnestock, M. (2012). Seasonal to decadal scale variations in the surface velocity of Jakobshavn Isbræ, Greenland: Observation and model-based analysis. Journal of Geophysical Research: Earth Surface, 117(2), 1–20. https://doi.org/10.1029/2011JF002110

Joughin, I., Smith, B. E., Howat, I. M., Scambos, T., & Moon, T. (2010). Greenland flow variability from ice-sheet-wide velocity mapping. Journal of Glaciology, 56(197), 415–430. https://doi.org/10.3189/002214310792447734.

Lucchitta, B. K., & Ferguson, H. M. (1986). Antarctica: measuring glacier velocity from satellite images. Science (New York, N.Y.), 234(4780), 1105–1108. https://doi.org/10.1126/science.234.4780.1105.

McMillan, M., Leeson, A., Shepherd, A., Briggs, K., Armitage, T. W. K., Hogg, A., Gilbert, L. (2016). A high resolution record of Greenland mass balance. Geophysical Research Letters, 43, 1–9. https://doi.org/10.1002/GRL.54619

McMillan, M., Shepherd, A., Gourmelen, N., Dehecq, A., Leeson, A., Ridout, A., Strozzi, T. (2014). Rapid dynamic activation of a marine-based Arctic ice cap. Geophysical Research Letters, 41, 8902–8909. https://doi.org/10.1002/2014GL062255.

Moon, T., Joughin, I., Smith, B., & Howat, I. (2012). 21st-century evolution of Greenland outlet glacier velocities. Science, 336(6081), 576–8. https://doi.org/10.1126/science.1219985

Moon, T., & Joughin, I. (2008). Changes in ice front position on Greenland's outlet glaciers from 1992 to 2007. Journal of Geophysical Research: Earth Surface, 113(2), 1–10. https://doi.org/10.1029/2007JF000927

Moon, T., Joughin, I., & Smith, B. (2015). Seasonal to multiyear variability of glacier surface velocity, terminus position, and sea ice/ice mélange in northern Greenland. Journal of Geophysical Research: Earth Surface, 120, 818–833. https://doi.org/10.1002/2015JF003494.

Moon, T., Joughin, I., Smith, B., Broeke, M. R., Berg, W. J., Noël, B., & Usher, M. (2014). Distinct patterns of seasonal Greenland glacier velocity. Geophysical Research Letters, 41, 7209–7216. https://doi.org/10.1002/2014GL061836.

Morlighem, M., Rignot, E., Mouginot, J., Seroussi, H., & Larour, E. (2015). IceBridge BedMachine Greenland, Version 2. Boulder, Colorado USA. NASA National Snow and Ice Data Center Distributed Active Archive Center. [09/08/2017]. http://dx.doi.org/10.5067/AD7B0HQNSJ29

Mouginot, J., Rignot, E., Scheuchl, B., Fenty, I., Khazendar, A., Morlighem, M., Paden, J. (2015). Fast retreat of Zachariæ Isstrøm, northeast Greenland. Science Express, 10.1126(November). https://doi.org/10.1126/science.aac7111

Münchow, A., Padman, L., & Fricker, H. A. (2014). Interannual changes of the floating ice shelf of Petermann Gletscher, North Greenland, from 2000 to 2012. Journal of Glaciology, 60(221), 489–499. https://doi.org/10.3189/2014JoG13J135

Münchow, A., Padman, L., Washam, P., & Nicholls, K. W. (2016). The ice shelf of Petermann Gletscher, North Greenland, and its connection to the Arctic and Atlantic Oceans. Oceanography, 29(4), 84–95. https://doi.org/10.5670/oceanog.2016.101

Nagler, T., Rott, H., Hetzenecker, M., Wuite, J., & Potin, P. (2015). The Sentinel-1 Mission: New Opportunities for Ice Sheet Observations. Remote Sensing, 7(7), 9371–9389. https://doi.org/10.3390/rs70709371

© Author(s) 2018. CC BY 4.0 License.

Nick, F. M., Luckman, a., Vieli, a., Van Der Veen, C. J., Van As, D., Van De Wal, R. S. W., … Floricioiu, D. (2012). The response of Petermann Glacier, Greenland, to large calving events, and its future stability in the context of atmospheric and oceanic warming. Journal of Glaciology, 58(208), 229–239. https://doi.org/10.3189/2012JoG11J242

Paul, F., Bolch, T., Kääb, A., Nagler, T., Nuth, C., Scharrer, K., Van Niel, T. (2015). The glaciers climate change initiative: Methods for creating glacier area, elevation change and velocity products. Remote Sensing of Environment, 162, 408–426. https://doi.org/10.1016/j.rse.2013.07.043

Rignot, E., & Mouginot, J. (2012). Ice flow in Greenland for the International Polar Year 2008-2009. Geophysical Research Letters, 39(11), 1–7. https://doi.org/10.1029/2012GL051634

Rignot, E., & Steffen, K. (2008). Channelized bottom melting and stability of floating ice shelves. Geophysical Research Letters, 35(2), 1–5. https://doi.org/10.1029/2007GL031765

Rignot, E., & Kanagaratnam, P. (2006). Changes in the Velocity Structure of the Greenland Ice Sheet. Science, 311(February), 986–990. https://doi.org/10.1126/science.1121381

Shepherd, A., Ivins, E. R., A., G., Barletta, V. R., Bentley, M. J., Bettadpur, S., Zwally, H. J. (2012). A Reconciled Estimate of Ice-Sheet Mass Balance. Science, 338(November), 1183–1189. https://doi.org/10.1126/science.1228102.

Strozzi, T., Luckman, A., Murray, T., Wegmuller, U., & Werner, C. L. (2002). Glacier motion estimation using SAR offset-tracking procedures. IEEE Transactions on Geoscience and Remote Sensing, 40(11), 2384–2391. https://doi.org/10.1109/TGRS.2002.805079

Studinger, M. S. 2014, updated 2016. IceBridge ATM L4 Surface Elevation Rate of Change, Version 1, Greenland subset. Boulder, Colorado USA. NASA National Snow and Ice Data Center Distributed Active Archive Center. doi: http://dx.doi.org/10.5067/BCW6CI3TXOCY. Accessed 5th July 2017.

Sundal, A. V., Shepherd, A., Van Den Broeke, M., Van Angelen, J., Gourmelen, N., & Park, J. (2013). Controls on short-term variations in Greenland glacier dynamics. Journal of Glaciology, 59(217), 883–892. https://doi.org/10.3189/2013JoG13J019

Tedesco, M., Fettweis, X., Mote, T., Wahr, J., Alexander, P., Box, J. E., & Wouters, B. (2013). Evidence and analysis of 2012 Greenland records from spaceborne observations, a regional climate model and reanalysis data. The Cryosphere, 7(2), 615–630. https://doi.org/10.5194/tc-7-615-2013

van den Broeke, M., Bamber, J. L., Ettema, J., Rignot, E., Schrama, E., van de Berg, W. J., … Wouters, B. (2009). Partitioning recent Greenland mass loss. Science, 326(November), 984–986. https://doi.org/10.1126/science.1178176

Van Der Veen, C. J., Plummer, J. C., & Stearns, L. A. (2011). Controls on the recent speed-up of Jakobshavn Isbræ, West Greenland. Journal of Glaciology, 57(204), 770–782. https://doi.org/10.3189/002214311797409776

Yague-Martinez, N., Prats-Iraola, P., Gonzalez, F. R., Brcic, R., Shau, R., Geudtner, D., Bamler, R. (2016). Interferometric Processing of Sentinel-1 TOPS data. IEEE Transactions on Geoscience and Remote Sensing, 54(4), 2220–2234. https://doi.org/10.1109/TGRS.2015.2497902

Zwally, H. J., Abdalati, W., Herring, T., Larson, K., Saba, J., & Steffen, K. (2002). Surface Melt – Induced Acceleration of Greenland Ice-Sheet Flow. Science, 297(July), 218–223. https://doi.org/10.1126/science.1072708.

The Cryosphere Discuss., https://doi.org/10.5194/tc-2017-251
Manuscript under review for journal The Cryosphere
Discussion started: 12 February 2018
© Author(s) 2018. CC BY 4.0 License.

7 Figures and Captions

- Figure 1. Time-averaged ice velocity magnitude maps for the period Oct/2014–Feb/2017 (a) Jakobshavn Isbræ (JI; 69°N, 50°W), (b) Petermann Glacier (PG; 81°N, 62°W), (c) Nioghalvfjerdsfjorden (79G; 79°N, 20°W) and Zachariæ Isstrøm (ZI; 78°N, 20°W) glaciers, derived from Sentinel-1 SAR images. Velocities are shown on a logarithm scale and overlaid on a SAR backscatter intensity image. The along-flow profiles are indicated by solid green lines scaled in kilometres, the solid white lines show the across-flow transects, the red triangles represent the locations at which velocity time series are extracted and the thick solid and dashed black lines represent the ice front locations (IF) and the grounding lines (GL), respectively. The inset figures show the location of each glacier.

- Figure 2. Average velocities extracted from along- and across-flow profiles of Jakobshavn Isbræ, Petermann Glacier, Nioghalvfjerdsfjorden and Zachariæ Isstrøm. Figures a–d present along-flow profiles of ice velocity (solid black lines), surface elevation from the GIMP DEM [Howat et al., 2014; dashed blue lines] and bed elevation from the IceBridge BedMachine Greenland V2 product [Morlighem et al., 2015; dashed yellow lines]. The location of each profile is shown in Figure 1 (green lines). The grey shaded area represents the floating regions, and the light grey dashed line the ice front positions. The blue, black and red markers represent the locations of the across-flow profiles. Figures e–h show the across-flow velocity profiles (solid white lines in Fig.1), centred on the main profile (solid green line).

- Figure 3. Time-averaged uncertainty in ice velocity at each site expressed in percentage, based on the signal to noise ratio (SNR) for (a) JI, (b) PG, and (c) 79G and ZI.

- Figure 4. Comparison between co-located and contemporaneous Sentinel 1-a/b and TerraSAR-X Jakobshavn Isbræ velocity measurements at Jif, J1 and J2 locations (blue, black and red dots respectively).

- Figure 5. Temporal evolution of Jakobshavn Isbræ (a) ice front position extracted from Joughin et al. [2014], ESA Greenland Ice Sheet Climate Change Initiative (CCI) project [2017], and Sentinel-1a/b SAR images represented in blue, black and magenta dots respectively, where higher values correspond to ice front retreat. Changes in ice velocity through time is also shown (b, c), extracted at the locations indicated in Figure 1. The velocity data derived from TerraSAR-X (Joughin et al., 2016) are shown as grey squares, and the data from Sentinel 1-a/b as coloured triangles.

- Figure 6. Comparison between Jakobshavn Isbræ ice velocity and calving front anomalies at the Jif site, 0.8 km upstream of the calving front, between 2009 and early 2017. Positive values correspond to ice front retreat and speed up respectively.

- Figure 7. Temporal evolution of ice velocity at the locations indicated in Figure 1 over (a) Petermann Glacier, (b) Nioghalvfjerdsfjorden and (c) Zachariæ Isstrøm. The data derived from TerraSAR-X [Joughin et al., 2016] and Sentinel 1-a/b are represented as grey squares and coloured triangles, respectively.

The Cryosphere Discuss., https://doi.org/10.5194/tc-2017-251
Manuscript under review for journal The Cryosphere
Discussion started: 12 February 2018
© Author(s) 2018. CC BY 4.0 License.

Figure 1

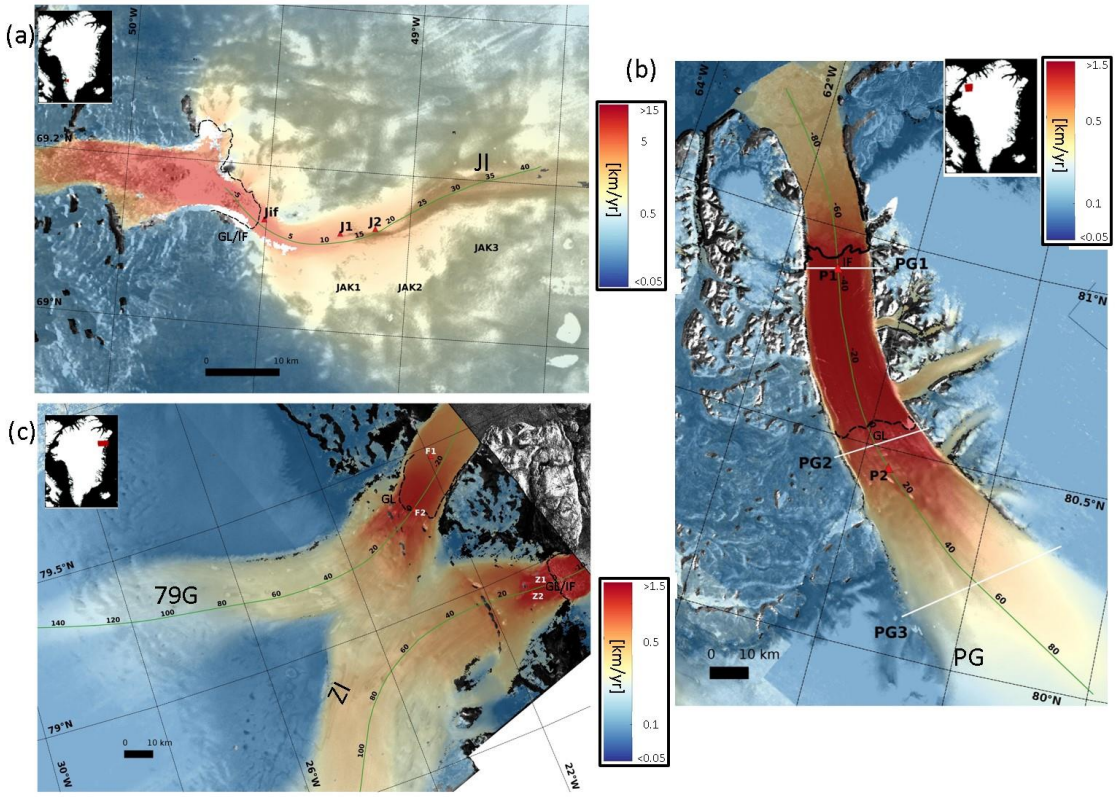

The Cryosphere Discuss., https://doi.org/10.5194/tc-2017-251
Manuscript under review for journal The Cryosphere
Discussion started: 12 February 2018
© Author(s) 2018. CC BY 4.0 License.

Figure 2

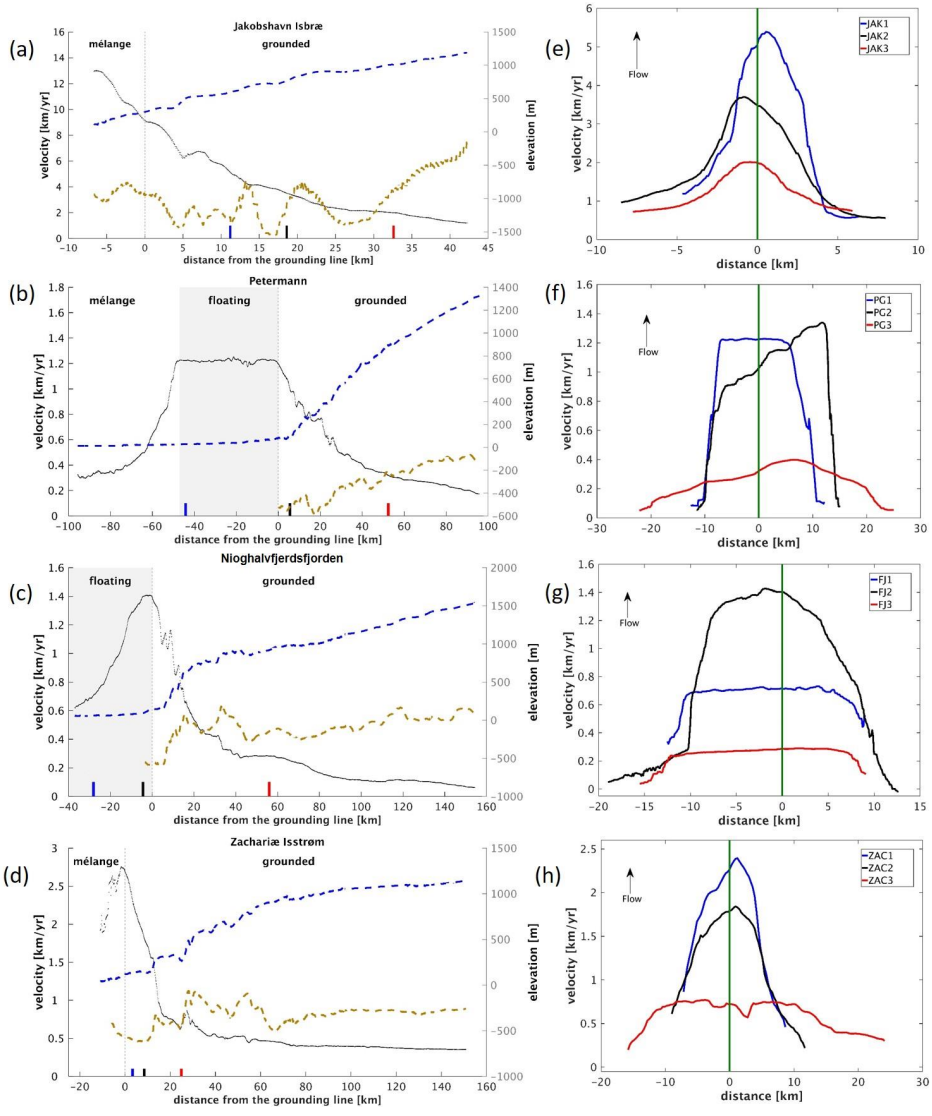

The Cryosphere Discuss., https://doi.org/10.5194/tc-2017-251
Manuscript under review for journal The Cryosphere
Discussion started: 12 February 2018
© Author(s) 2018. CC BY 4.0 License.

Figure 3

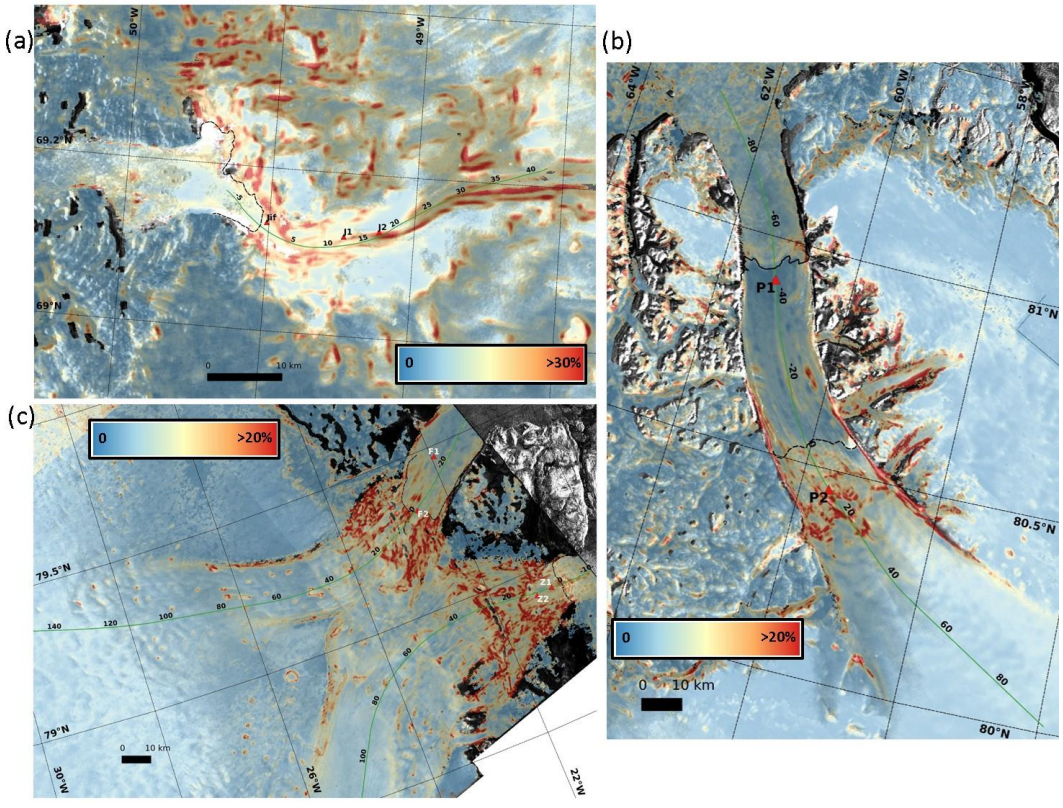

The Cryosphere Discuss., https://doi.org/10.5194/tc-2017-251
Manuscript under review for journal The Cryosphere
Discussion started: 12 February 2018
© Author(s) 2018. CC BY 4.0 License.

Figure 4

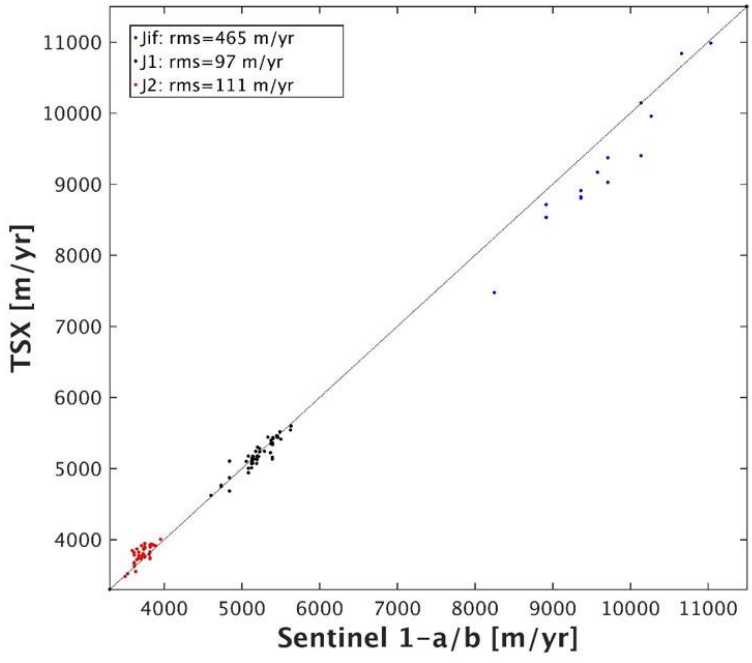

The Cryosphere Discuss., https://doi.org/10.5194/tc-2017-251
Manuscript under review for journal The Cryosphere
Discussion started: 12 February 2018
© Author(s) 2018. CC BY 4.0 License.

Figure 5

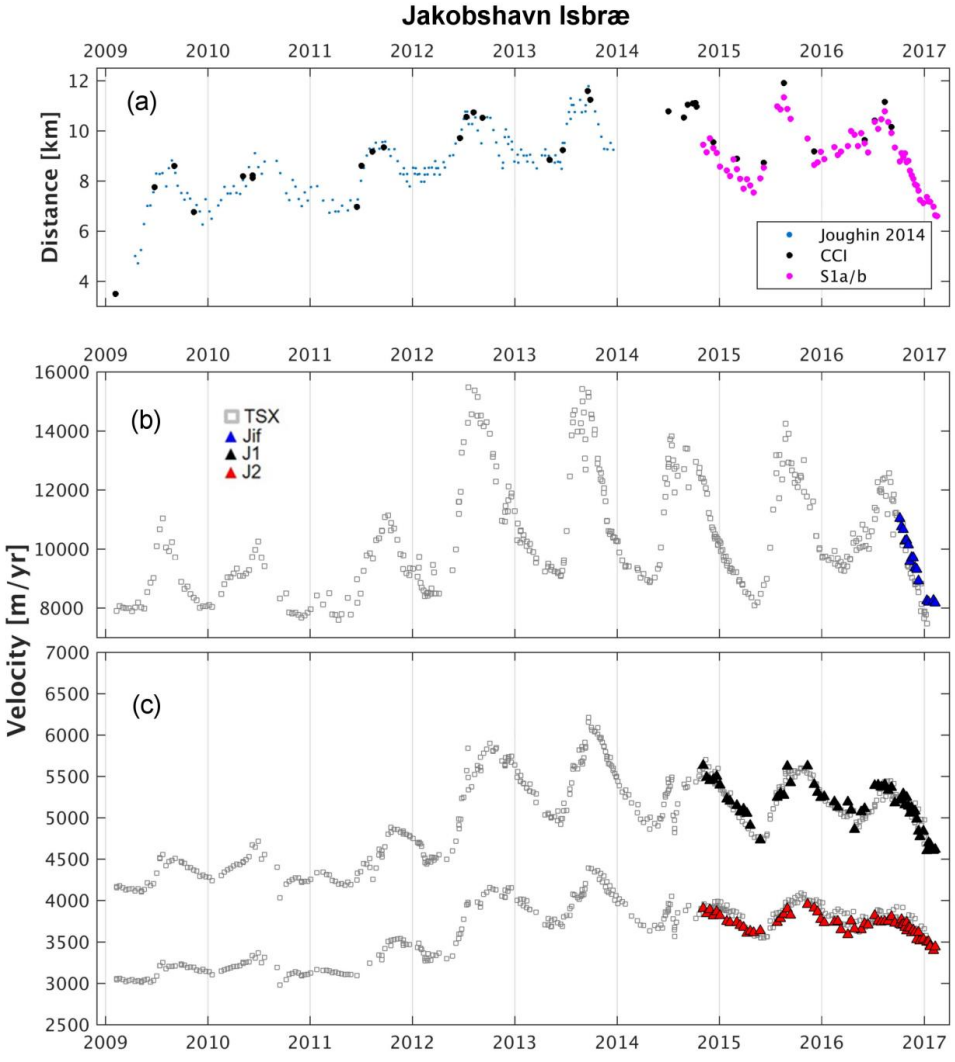

The Cryosphere Discuss., https://doi.org/10.5194/tc-2017-251
Manuscript under review for journal The Cryosphere
Discussion started: 12 February 2018
© Author(s) 2018. CC BY 4.0 License.

Figure 6

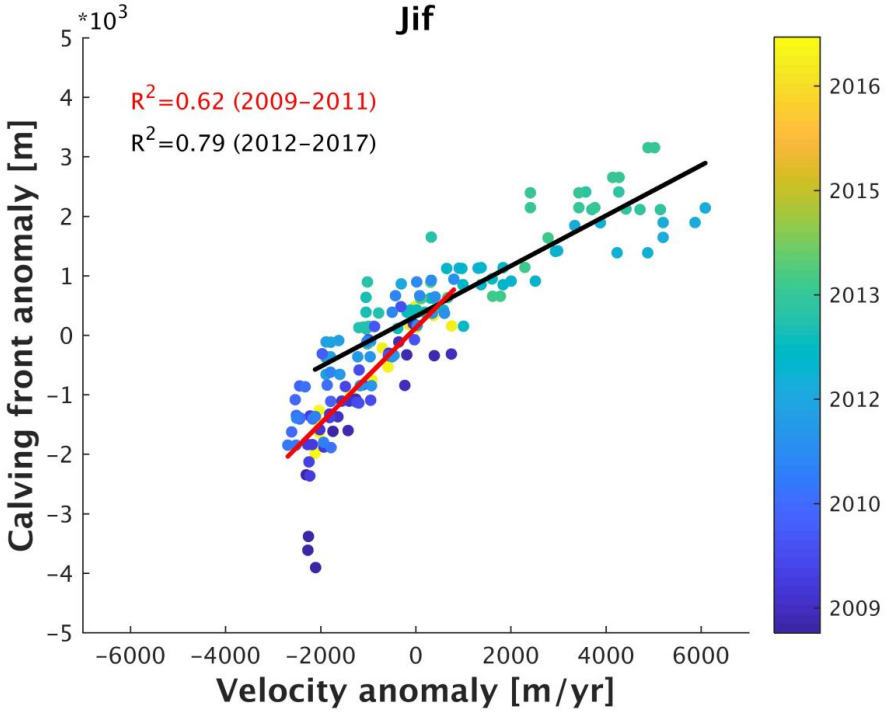

The Cryosphere Discuss., https://doi.org/10.5194/tc-2017-251
Manuscript under review for journal The Cryosphere
Discussion started: 12 February 2018
© Author(s) 2018. CC BY 4.0 License.
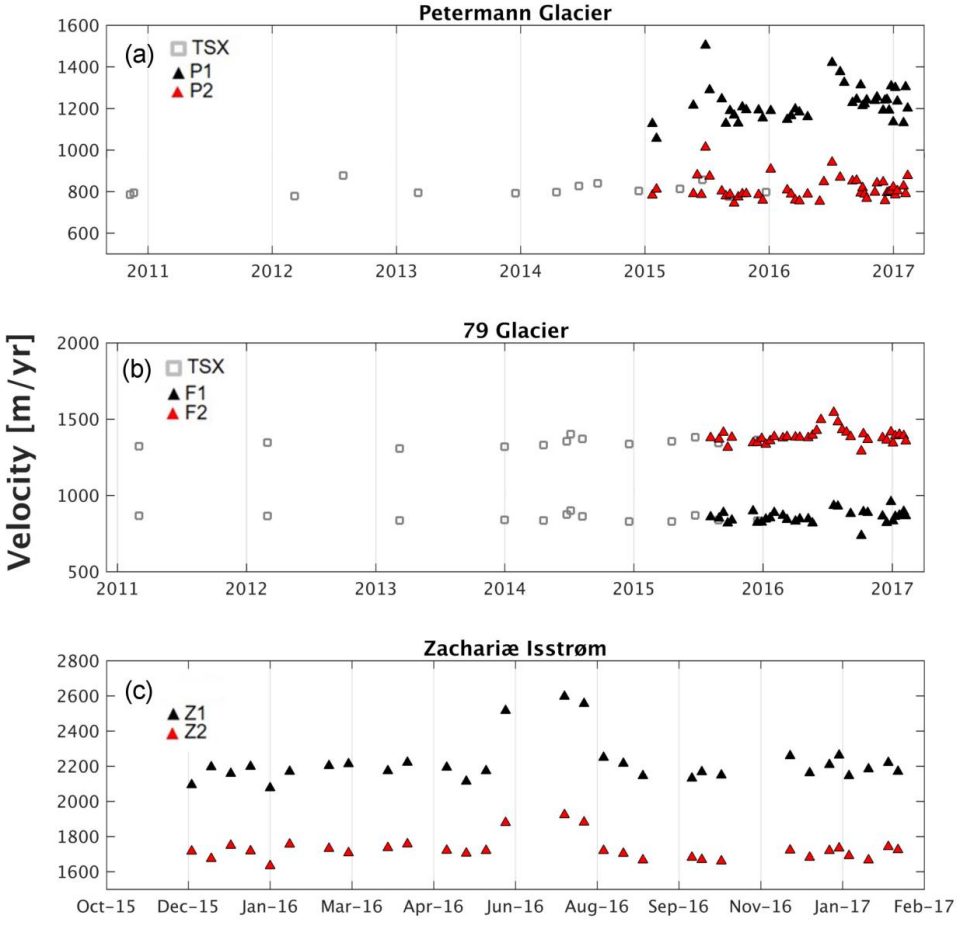
Figure 7